JOURNAL OF MATERIALS SCIENCE 24 (1989) 1757-1766

Preparations and characterization of lanthana catalysts: study of their activity in CO/H_2 reactions

D. ANDRIAMASINORO, R. KIEFFER, A. KIENNEMANN,
J. L. REHSPRINGER*, P. POIX*
Laboratoire de Chimie Organique Appliquée, UA CNRS 469,
*and *Département Sciences des Matériaux, UA CNRS 440, EHICS, 1, rue Blaise Pascal,*
67008 Strasbourg, France

A. VALLET, J. C. LAVALLEY,
Laboratoire de Spectrochimie, UA CNRS 414, IMSRA, 14032 Caen, France

Two original methods of preparation of lanthana with hexagonal structure as well as the stabilization of its cubic structure by addition of yttria were investigated. The physical properties and the catalytic behaviour of these samples are compared with classical preparations. The influence of the preparation techniques and of the pretreatment on the specific area, morphology and chemisorption of probe molecules were tested, the latter using mainly Fourier transform infrared spectroscopy. Catalytic tests, operated at high $CO-H_2$ pressure and high temperature, led to the classical isosynthesis product distribution. The prepared lanthana samples are active in the hydrogenation of carbonate to formate species which can be involved in the formation of formaldehyde in the first step of the isosynthesis reaction. The evolution of the oxide catalysts to hydrates and carbonates during the reaction was studied.

1. Introduction

Until recently, the catalysis of rare earths oxides had essentially focused on their dehydration, dehydrogenation and aldolization activities [1-3]. Taking into account earlier results based on thoria [4-7], the potentialities of rare earths oxides, used alone, in $CO-H_2$ synthesis, has recently been demonstrated [8, 9]. Since Ichikawa's studies [10-12] on transition metal-impregnated lanthanum oxide, the interest in rare earth oxides has increased in a tremendous way. Their promotor effect in alcohol synthesis (methanol, ethanol) can be related to an unusual CO chemisorption [13, 14] and/or their interaction with various intermediate species, and shows their novel features when compared to more conventional supports like SiO_2 or Al_2O_3.

To explain this peculiar behaviour, it has been suggested that their reactivity with water [3, 15, 16] combined with various treatments during the reduction of supported metals [17] may well be the key to their activity. Recently, it was shown that atmospheric CO_2 [18, 19] not only converts lanthanum oxide into surface carbonates but also into bulk carbonates.

This led Bernal *et al.* [19] to persue exhaustive studies on the ternary $Ln_2O_3-CO_2-H_2O$ system. However, to our knowledge, only a few works have been devoted to the influence of the preparation methods of rare earth oxides, on their physical properties and catalytic behaviour in $CO-H_2$ synthesis.

The aim of the present work was to compare the effect of various preparation methods on the physical properties (e.g. chemisorption of some molecules such as H_2O, CO_2, CH_3OH) and catalytic activity in isosynthesis. Several techniques have been used: thermogravimetric analysis (TGA), X-ray diffraction (XRD), electron microscopy, Fourier transform infrared (FT-IR) spectroscopy, chemical trapping and high-pressure reactions.

2. Experimental procedure

2.1. X-ray spectra and TGA

A Siemens D500 device has been used for the X-ray diffraction analysis. The end point of the heating treatment is determined by a SETARAM B 60 thermogravimetric apparatus.

2.2. FT-IR

Spectra have been recorded at room temperature using a Nicolet FT-IR spectrometer. Oxides were used as self-supporting wafers and activated *in situ* under vacuum at 550 or 750° C, except in one case in which the samples were mixed with KBr (5 wt %) to record their spectra without activation. CO_2, H_2O, CH_3OH and $CH_3{}^{18}OH$ were introduced at room temperature on the activated samples.

2.3. Chemical trapping

The concentration of surface formate species was measured by the conventional chemical trapping (using dimethylsulphate as trapping reagent) [20]

0022-2461/89 $03.00 + .12

after batch reaction of the CO/H_2 mixture with the catalyst.

2.4. High-pressure reactions

The high-pressure reactions were performed in a stainless steel reactor which can withstand pressures up to 550 bar. Total conversion, efficiency and selectivity were measured by G.C. Reaction procedures and analytical details are given by Kieffer *et al.* [8, 9].

The following symbolism will be used throughout this paper for La_2O_3. La_2O_3 ex nitrate: calcination of $La(NO_3)_3 \cdot 6H_2O$. La_2O_3 ex ammonia: precipitation by ammonia. La_2O_3 hydrazine: chelation of lanthanum salts by hydrazine hydrate. La_2O_3 ex ethoxide: hydrolysis of $La(C_2H_5O)_3$. La_2O_3 cubic phase or yttrium-doped La_2O_3: La_2O_3–Y_2O_3 solid solutions.

3. Results and discussion

3.1. Preparation of lanthanum oxide in a hexagonal cell

Two conventional methods were used: thermal decomposition of lanthanum nitrate, and pyrolysis of lanthana hydroxide obtained by ammonia precipitation of aqueous solutions of lanthanum salts (nitrate) (Fig. 1a).

Attempts were also made to prepare oxides with various morphologies by thermal decomposition of a lanthanum chelate or by drying of a sol/gel process lanthanum hydroxide. On the other hand, the addition of yttria changes the hexagonal structure of La_2O_3 towards a cubic cell.

3.1.1. Lanthanum alcoxide preparation and hydrolysis

The preparation of lanthanum alcoxide is often difficult because of its high sensitivity to water. It is necessary to work in a perfectly anhydrous solvent. Lanthanum nitrate must first be dried at 110° C over 24 h. Lanthanum nitrate is then treated by sodium ethylate in ethanol solution and nitrate is exchanged by the ethoxy group as follows:

$$2La\,(NO_3)_3 + 3C_2H_2ONa \longrightarrow La(OC_2H_5)_3 + \text{“}La(NO_3)_3,\ 3NaNO_3\text{”}$$

The composition of the complex “$La(NO_3)_3$, $3NaNO_3$” was determined by atomic absorption. Lanthanum alcoxide is then filtered off and hydrolysed by an excess of water-diluted ethanol.

$$La(OC_2H_5)_3 + 3H_2O \rightarrow La(OH)_3 + 3C_2H_5OH$$

Lanthanum hydroxide, a white powder called gel, is dried in a CO_2-free atmosphere to avoid undesired carbonation. Chemical analysis shows less than 1 mol % sodium in the powder.

La_2O_3 with a well-crystallized structure (Fig. 1b) appears only after heat treatment at 800° C. Despite a weak specific area of $24\,m^2\,g^{-1}$ at 600° C, a mean particle of $\sim 0.2\,\mu m$ has been measured by scanning electron microscopy (SEM) (Fig. 2a).

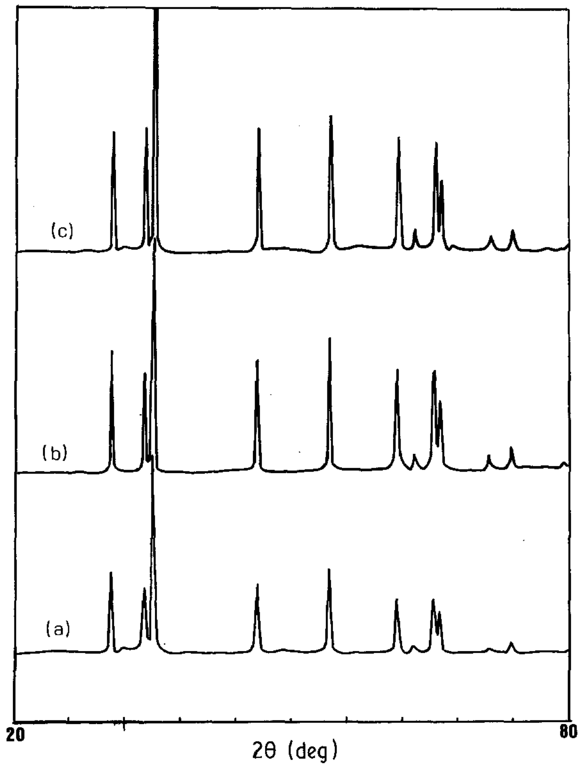

Figure 1 X-ray pattern of lanthana samples. (a) La_2O_3 ex-ammonia, (b) La_2O_3 ex-ethoxide, (c) La_2O_3-hydrazine.

3.1.2. Hydrazine hydrate–lanthana chelate formation

Hydrazine hydrate is added to a lanthanum nitrate solution, and a rubber-like paste is formed. The thermal decomposition of this chelate with a complex structure was investigated. Weight losses corresponding to the decomposition of the probably hydrated chelate are observed. Above 600° C, no further weight loss is noticed and X-ray patterns show the appearance of hexagonal La_2O_3 (Fig. 1c). The specific area was $\sim 3\,m^2\,g^{-1}$. SEM analysis reveals small platelets of about $5\,\mu m$ composed by an agglomeration of little particles of about $0.2\,\mu m$ (Fig. 2b).

Thermogravimetric analysis (Fig. 3) of the oxides prepared in different ways is at variance with that of sol/gel preparations (e.g. number and temperature of decomposition steps). The last step can correspond to the decomposition of a carbonate phase, and has a different importance depending on the preparation method. Indeed hexagonal La_2O_3 is highly sensitive to carbonation and hydration.

3.1.3. Preparation of lanthanum oxide in a cubic cell

The aim of this preparation was to try to avoid carbonation of lanthanum oxide. The chosen way was to prepare a solid solution between La_2O_3 and Y_2O_3. This material is obtained by ammonia precipitation of an aqueous solution of lanthanum and yttrium nitrate. Two compositions were used: 0.8 La_2O_3–0.2 Y_2O_3, and 0.5 La_2O_3–0.5 Y_2O_3. For 0.8 La_2O_3–0.2 Y_2O_3 the stability of the pseudocubic phase was found for a heat treatment between 500 and 600° C (2 h). This temperature is in accordance with the isosynthesis process conditions.

The observed X-ray patterns show broad lines which are characteristic of a low crystallinity. In Table I, the

TABLE I X-ray data on $0.8La_2O_3$–$0.2Y_2O_3$

hkl	d_{mes} (nm)	d_{cal} (nm)	Intensity
222	0.327	0.330	F
400	0.287	0.287	M
440	0.203	0.203	f
622	0.172	0.173	tf.

TABLE II X-ray data on $0.5La_2O_3$–$0.5Y_2O_3$

hkl	d_{mes} (nm)	d_{cal} (nm)	a (nm)
222	0.3148	0.3146	1.0905
400	0.2725	0.2725	1.0902
440	0.1926	0.1926	1.0895
622	0.1642	0.1642	1.0892

computed and measured d_{hkl} data of a quadratic cell ($a = 1.148$ nm and $c = 1.135$ nm) are compared.

This 0.8 La_2O_3–$0.2Y_2O_3$ phase is metastable. At temperatures above 600° C, separation occurs, and a hexagonal La_2O_3 cell and pseudocubic phase still richer in yttria are observed.

$$0.8\ La_2O_3\text{–}0.2\ Y_2O_3 \xrightarrow{T>600^\circ C} xLa_2O_{3hex}$$
$$+\ 1 - x[La_{(1.6-2x)/1-x}Y_{0,4/1-x}O_3]$$

The pseudocubic structure is characterized by the decrease in the c/a ratio when the secondary phase is enriched in Y_2O_3. The c/a ratio of 1.013 at 600° C drops to 1.002 at 900° C. Thus the stabilizing effect of Y_2O_3 for the cubic cell of Y_2O_3–La_2O_3 solid solution is well established. Heat treatment above 900° C leads to the formation of a stable ternary phase of perovskite nature (Fig. 4b). The separation phenomenon is irreversible. For 0.5 La_2O_3–0.5 Y_2O_3 the cubic phase appears at 680° C (Fig. 4a). Its cell parameter is 0.1090 ± 0.0005 nm (Table II).

It can be noticed that this cubic phase is transformed into a perovskite $LaYO_3$ by heat treatment above 1000° C.

3.2. FT-IR studies of surface properties of La_2O_3

Carbonation and hydration phenomena have been mainly studied. Figs 5 to 7 show the spectra of the four preparations (ex-ethoxy, ex-nitrate, hydrazine and $0.8La_2O_3$–$0.2Y_2O_3$ cubic sample). These four samples were analysed either at room temperature (in KBr mixture) or after activation at 550 and 750° C.

Three regions can give important results: from 4000 to 3000 cm^{-1} corresponding to ν(OH) and $\nu(H_2O)$ vibrations, from 1600 to 1250 cm^{-1} corresponding to $\nu(CO_3^{2-})$ vibrations [3, 17, 19, 21]; from 1000 to 500 cm^{-1} corresponding to the oxide vibrations bands.

In Fig. 5, a sharp absorption band at 3610 cm^{-1} and a broad band of lower intensity at 3450 to 3460 cm^{-1} are observed for ex-ethoxide, ex-ammonia and hydrazine samples. For the yttria-doped samples, two bands at 3610 and 3590 cm^{-1} are superimposed and the 3440 to 3460 cm^{-1} band can hardly be observed. In the 1000 to 500 cm^{-1} region, in addition to bands at 850 and 855 cm^{-1}, a band at 650 cm^{-1} (640 cm^{-1} [19]) appears. A good relation exists between its intensity and that of the 3610 cm^{-1} for the ex-ethoxide, ex-ammonia and hydrazine samples. For the yttrium-doped sample, the broad band at 3590 cm^{-1} enhances the intensity of the 3610 cm^{-1} band and this must be taken into account.

The band situated at 3610 cm^{-1} has been attributed to a hydroxide phase and that at 650 cm^{-1} to a deformation mode of La–OH in the corresponding hydroxide [18, 22, 23].

Two very strong absorption bands are observed at near 1470 and 1390 cm^{-1} (Fig. 6). They are due to carbonate species. The comparative study of the accompanying weak bands according to the sample allows classification of them into two groups corresponding to two different types of adsorbed species:

Species A, characterized by very sharp bands at 2580, 2540, 2520, 1830, 1730, 1085 and 855 cm^{-1} (very clear for La_2O_3 ex-ethoxy);

Species B, which gives rise to broader bands at 1760, 1060, 855 cm^{-1}, which appear essentially for the La_2O_3 hydrazine and for the yttria-doped samples.

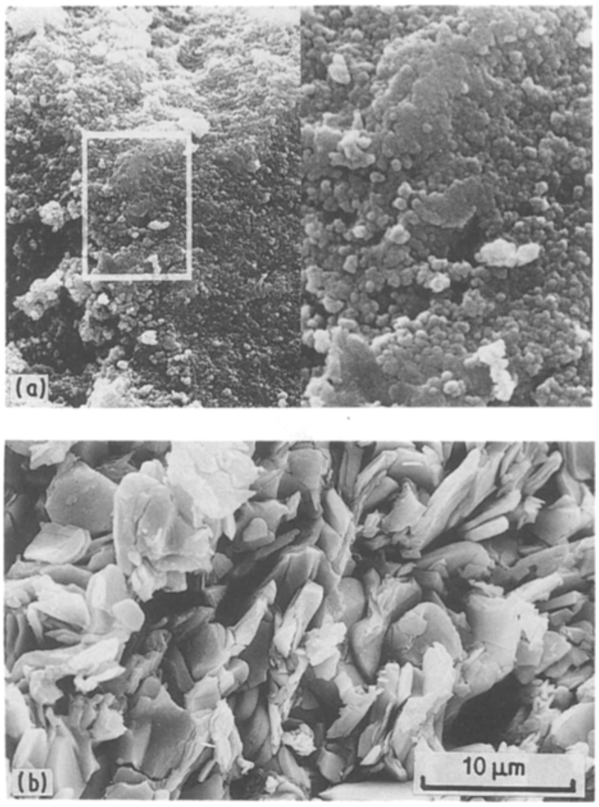

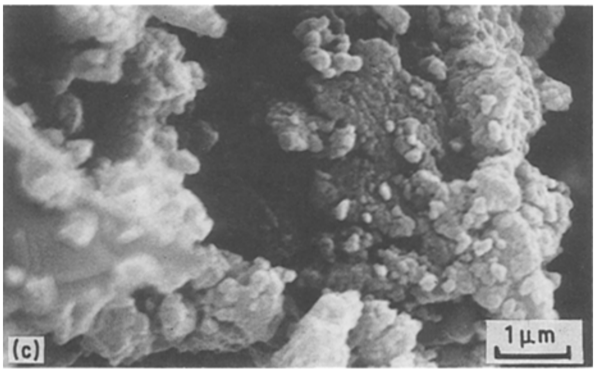

Figure 2 SEM data. (a) La_2O_3 ex-ethoxide, (b) La_2O_3 hydrazine, (c) La_2O_3 hydrazine after CO + H_2 reaction.

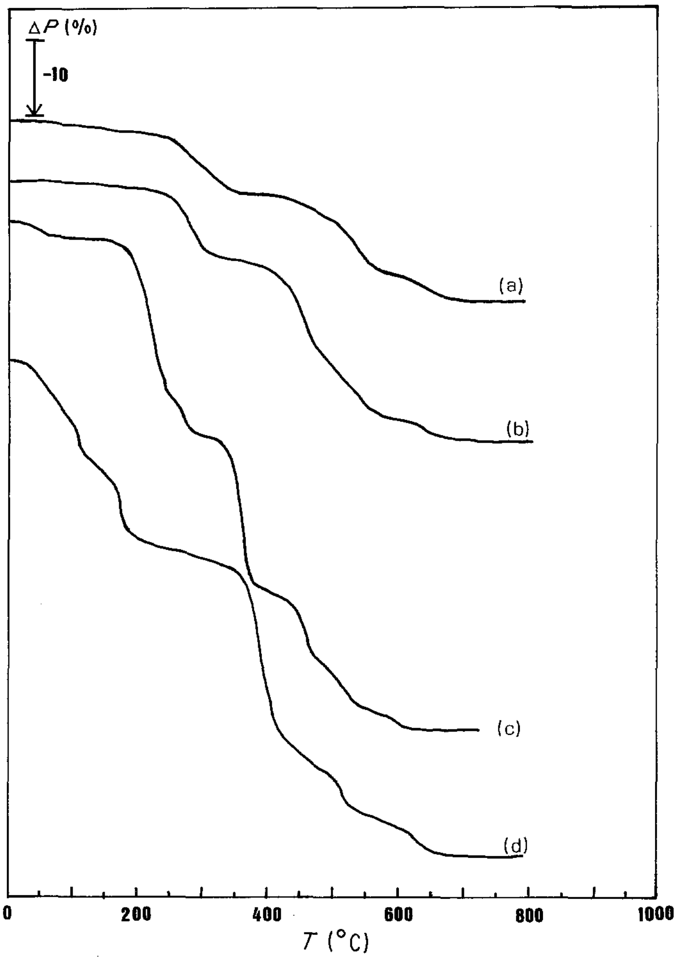

Figure 3 TG curves of lanthana samples. (a) La_2O_3 ex-ethoxide, (b) La_2O_3 ex-ammonia, (c) La_2O_3-hydrazine, (d) La_2O_3 ex-nitrate.

Without more details, the bands of groups A and B can be ascribed to two different types of carbonates. According to Bernal *et al.* [24], the shift of the band situated at $1090\,cm^{-1}$ to $1070\,cm^{-1}$ (1085 and $1060\,cm^{-1}$ in our case) is characteristic of a new carbonate phase. After heating at 550° C, the carbonate band intensity decreases as follows

$$\text{yttria-doped} > La_2O_3 \text{ ex-ethoxide}$$
$$> La_2O_3 \text{ ex-ammonia} > La_2O_3 \text{ hydrazine}$$

After heating at 750° C, only carbonates on the yttria-doped solid remain. The hypothesis of bands attributed to nitrates can be discarded [25].

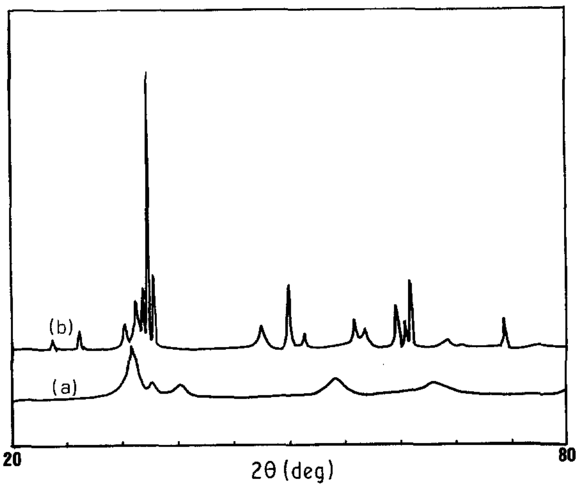

Figure 4 X-ray pattern of La_2O_3–Y_2O_3, after treatment at (a) 680° C, (b) 1000° C.

3.2.1. CO_2 adsorption

To confirm these band attributions, CO_2 was adsorbed on an ex-ethoxide sample activated at 750° C (Fig. 8). Two broad bands appear at 1490 and $1400\,cm^{-1}$ near to those observed on La_2O_3 hydrazine (Fig. 5).

Bands of weaker intensity around 1060, 850 and $750\,cm^{-1}$ (broad) corresponding to species B are observed. The same bands are obtained when La_2O_3 ex-ethoxide activated at 750° C is exposed to air at room temperature (Fig. 9).

Bands in the 1400 to $1500\,cm^{-1}$ region are not characteristic of surface carbonates but rather of polydentate bulk carbonates [21] according to Bernal *et al.* [18]. However, Rosynek [3] attributed them to monodentate surface carbonates.

With the exception of perhaps a band at about $1230\,cm^{-1}$ on the La_2O_3 hydrazine, no hydrogenocarbonates are observed.

3.2.2. H_2O adsorption

On La_2O_3 ex-ethoxide, adsorption of water in slight amounts ($\simeq 2$ torr at room temperature) results in a sharp band at $3700\,cm^{-1}$, and of a broad band at $3550\,cm^{-1}$ with a shoulder at $3400\,cm^{-1}$ (Fig. 10). A band at $1650\,cm^{-1}$ shows that at least part of the water is molecularly adsorbed. A band at $630\,cm^{-1}$ can be attributed to the δ(OH) vibration of bonded hydroxyl groups [18, 22, 23].

After heating at 360° C and evacuation, only two bands remain: νOH at $3660\,cm^{-1}$ (sharp), and νOH at $3580\,cm^{-1}$ (broad). They are characteristic of νOH vibrations of surface hydroxyl groups. This attribution

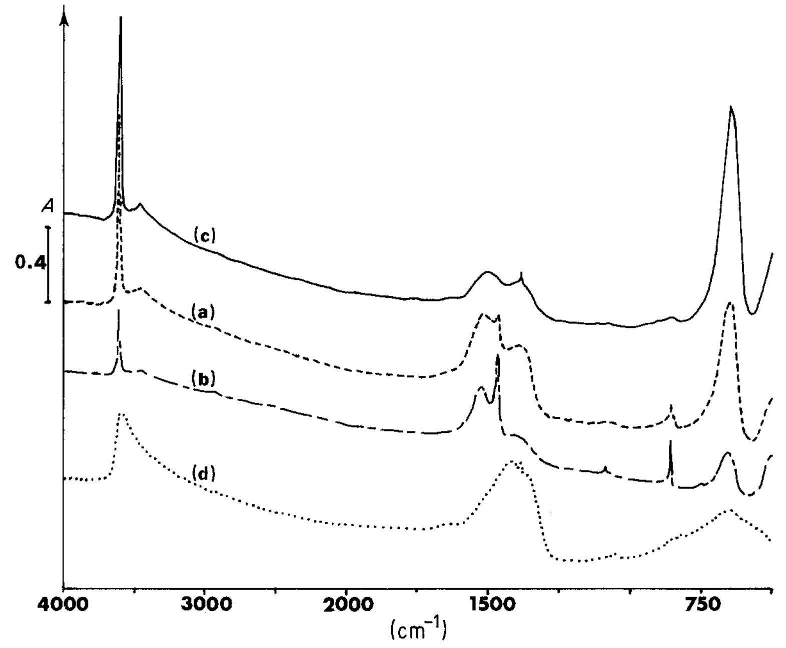

Figure 5 FT-IR spectra of lanthana sample in KBr. (a) (– – –) La_2O_3 ex-ammonia, (b) (– – –) La_2O_3 ex-ethoxide, (c) (——) La_2O_3-hydrazine, (d) (· · · ·) La_2O_3–Y_2O_3.

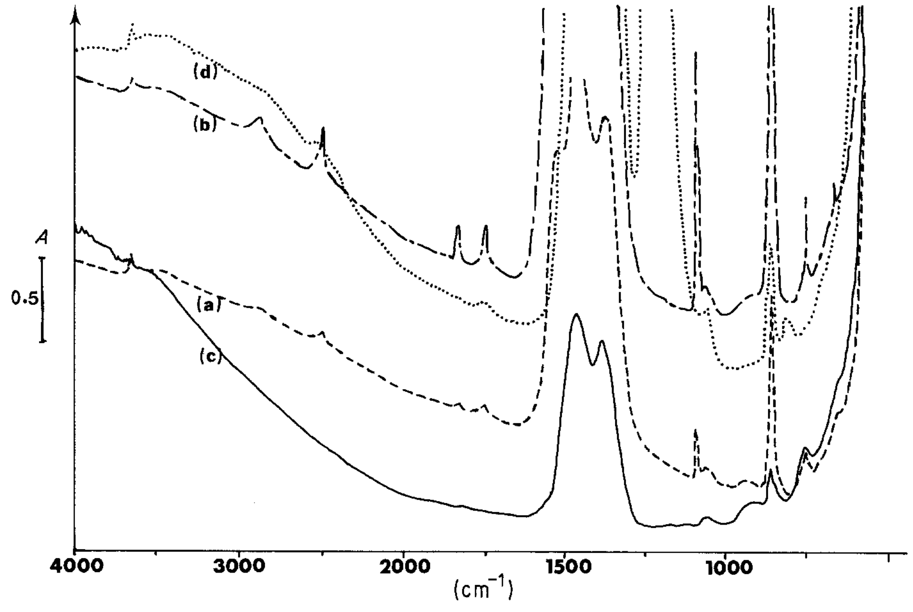

Figure 6 FT-IR spectra of lanthana activated at 550° C. (a) (– – –) La_2O_3 ex-ammonia, (b) (– – –) La_2O_3 ex-ethoxide, (c) (——) La_2O_3-hydrazine, (d) (· · · ·) La_2O_3–Y_2O_3.

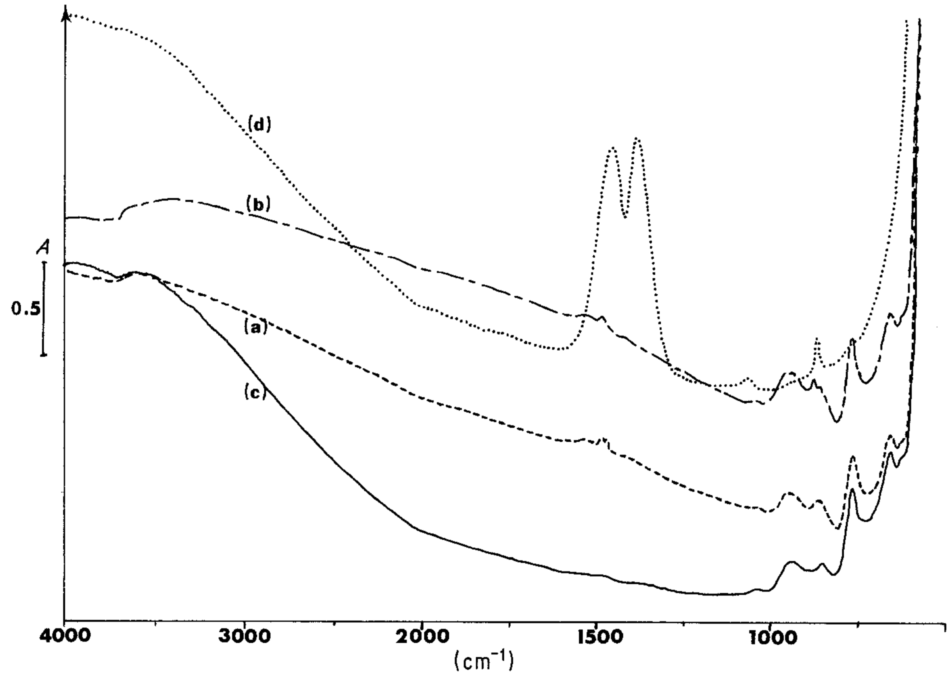

Figure 7 FT-IR spectra of lanthana activated at 750° C. (a) (– – –) La_2O_3 ex-ammonia, (b) (– – –) La_2O_3 ex-ethoxide, (c) (——) La_2O_3-hydrazine, (d) (· · · ·) La_2O_3–Y_2O_3.

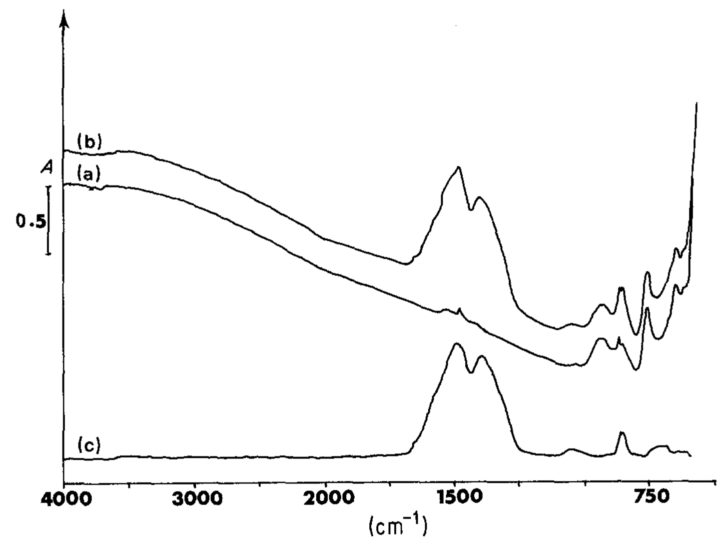

Figure 8 FT-IR spectra. Adsorption of CO_2 on La_2O_3 sample. (a) La_2O_3 ex-ethoxide after activation at 750° C. (b) CO_2 (100 mol g^{-1}) at room temperature. (c) Difference (b)–(a).

will be more precisely explained by methanol adsorption. Furthermore, yttria-doped samples are less sensitive to hydration at low pressure. This lower sensitivity is one of the subjects under investigation in this study.

3.2.3. *Methanol adsorption*

After activation at 550° C, methanol was introduced at room temperature on the four samples. The excess of methanol was then evacuated (Fig. 11). Identical bands are found for the four samples.

In the νCH_3 range (2700 to 3000 cm^{-1}) the most intense band is situated at 2780 cm^{-1}. Such a low wave number can be related to the basicity of the oxide. The most striking point is the appearance of several ν(CO) methoxy bands between 1200 and 1000 cm^{-1}: 1120 (sharp), 1075 with a shoulder at 1060 cm^{-1}. When compared with studies on MgO, ZrO_2, ThO_2 and CeO_2 [26–28] the band at 1120 cm^{-1} can be ascribed to a monodentate methoxy. The band at 1075 cm^{-1} is characteristic of a bidentate methoxy. To these two bands must correspond two νOH vibrations: monodentate (not easily observable) and bidentate at 3660 cm^{-1}. In Fig. 11, rationalized to the unit mass of the substrate, it can be seen that the surface sites are the most abundant on the ex-ethoxide and ex-ammonia samples.

$CH_3\,^{18}OH$ (92% isotopic purity) has been adsorbed on La_2O_3 ex-ethoxy activated at 750° C (Fig. 12) to prove that methanol adsorption indeed occurs by breaking the OH bond. Two bands are observed at 1085 and 1056 cm^{-1}. The isotopic effect (33 and 29 cm^{-1}, respectively) shows that the two types of methoxy species result from the cleavage of the OH bond of methanol.

3.2.4. *Results relative to formate species*

For the yttria-doped La_2O_3 activated at 750° C, introduction of H_2 (200 torr at 220° C) results in a slight decrease of the carbonate bands while a band appears at 1570 cm^{-1} which can be attributed to a formate species. The reaction of carbonates with hydrogen to give formates is important in CO–CO_2–H_2 systems [29] because formates are the most commonly admitted intermediates on metal oxides to lead to methanol.

The formate entities have been characterized on various catalytic substrates [20] and the highest concentration after CO–H_2 reaction found by chemical trapping is observed on La_2O_3 ex-ethoxide pretreated before reaction at 800° C (7.4×10^{-5} mol/g cat.). On La_2O_3 hydrazine, this concentration is about 3.5×10^{-5} mol/g cat. This is in agreement with the FT-IR

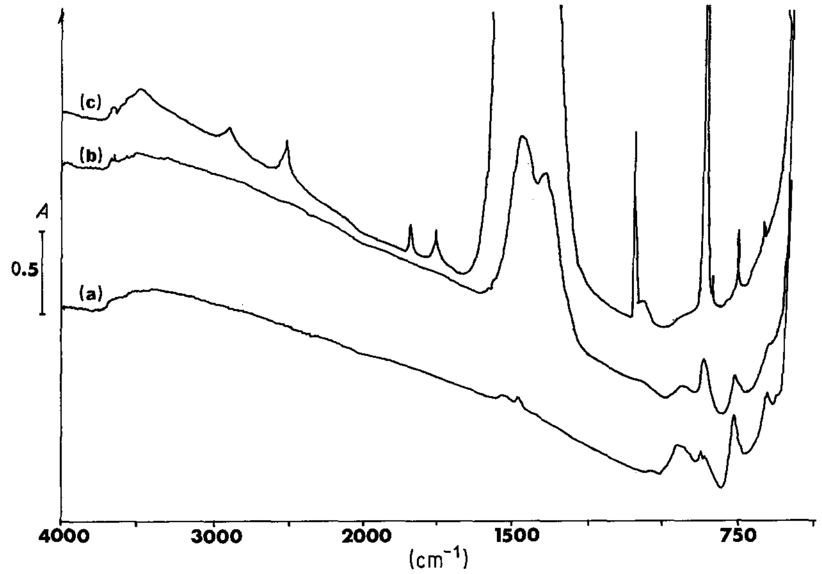

Figure 9 FT-IR spectra: effect of air carbonation. (a) La_2O_3 ex-ethoxide after activation at 750° C. (b) After air carbonation at room temperature (24 h) and retreatment at 550° C. (c) La_2O_3 ex-ethoxide after activation at 550° C.

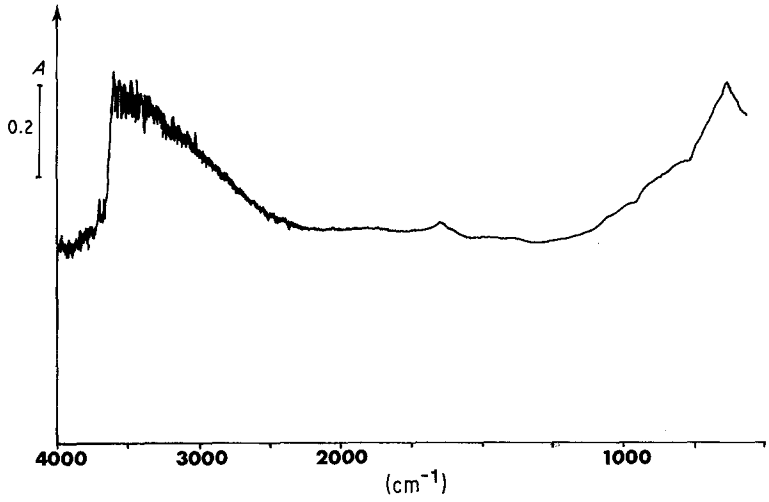

Figure 10 Effect of H_2O (2 torr) addition at room temperature on La_2O_3 ex-ethoxide activated at 750° C.

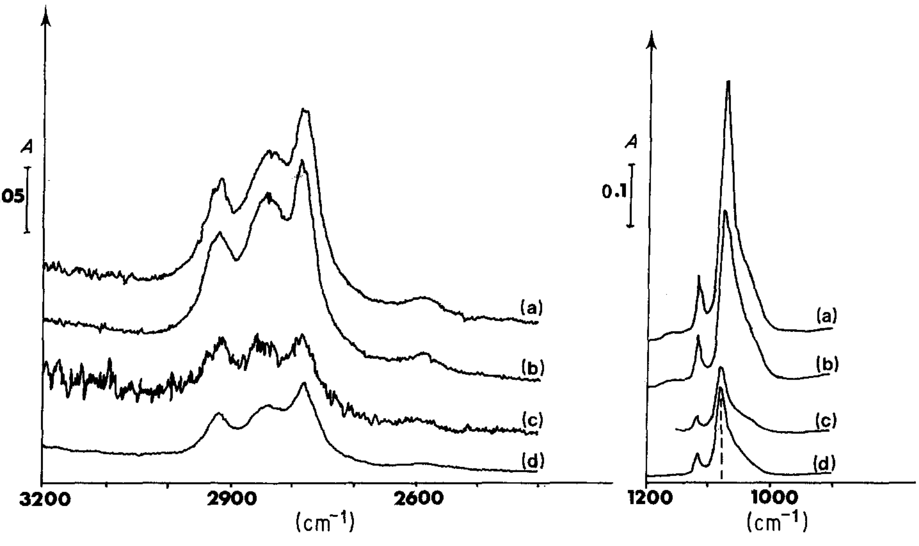

Figure 11 FT–IR spectra: addition of CH_3OH at room temperature on: (a) La_2O_3 ex-ethoxide; (b) La_2O_3 ex-ammonia; (c) La_2O_3-Y_2O_3; (d) La_2O_3 hydrazine activated at 550° C.

studies which indicates that the surface sites are more numerous on La_2O_3 ex-ethoxide.

3.3. CO–H_2 synthesis results

The isosynthesis reaction is performed in the conditions given in [8, 9]: $T = 475°$ C, $P = 400$ bar, CO/H_2 = 1, G.S.V.H. = 2000. Liquids are analysed after 24 h unless otherwise stated.

The results are given in Tables III to VI. The calcination temperatures were chosen on the basis of the results of the TG curves of the air-heated samples (Fig. 3).

In all cases, the product distribution is in agreement with previous results [8, 9] and shows important differences from a classical distribution in CO–H_2 synthesis given by the so-called Anderson–Schulz–Flory repartition (Fig. 13). This distribution can be explained on the basis of an aldolization growing mechanism [8, 9].

Table III gives the results related to the preparation method. All the samples were pretreated at 800° C. Unlike as suggested by FT–IR and chemical trapping experiments, no important difference could be observed.

Table IV shows the changes occurring with variation

TABLE III Reactivity of lanthana in the CO–H_2 reaction: influence of the preparation method

Catalyst	Area ($m^2 g^{-1}$)	Conversion (%)			Selectivity RH					Selectivity ROH			Ratio iso C_4/C_4 (%)	Conversion iso C_4 (%)
		RH	ROH	CO_2	C_1	C_2	C_3	C_4	C_5^+	DME	MeOH	iC_4OH		
La_2O_3 ex-ammonia 800° C	5	6.8	0.8	10	25	14	13	22	15	9	1	1	67	1.2
La_2O_3 ex-nitrate 800° C	4.8	6.8	2.9	10.9	19.1	14.9	10.6	20.2	5.2	14.5	12	2.8	69	1.5
La_2O_3 ex-ethoxy 800° C	4	4	1.6	8	19	14	9	23	7	15	9.3	4	62	1
La_2O_3-hydrazine 800° C	3	3	1.2	6.4	21.1	12.3	11.7	16.5	10	10.2	12.1	5.4	73	0.6

$P = 400$ bar; $T = 475°$ C; CO/H_2 = 1; G.S.V.H. = 2000; time 24 h; pretreatment 800° C.

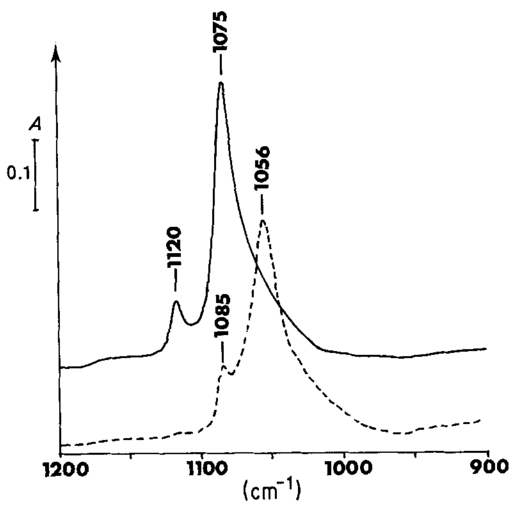

Figure 12 FT-IR spectra: comparison between $CH_3\,^{16}OH$ and $CH_3\,^{18}OH$ adsorption. (a) La_2O_3 ex-ethoxide activated at 750° C + $CH_3\,^{16}OH$; (b) La_2O_3 ex-ethoxide activated at 750° C + $CH_3\,^{18}OH$.

of calcination temperature. Too high a calcination temperature is detrimental to a high conversion and for the formation of iso C_4 compounds.

The influence of the change from an hexagonal to a cubic structure is given in Table V.

For a La/Y ratio of 1, the activity is enhanced by increasing the formation of methane and ethane, but the conversion to iso C_4 is lowered.

The ageing of the catalyst (Table VI) led to a similar behaviour of the different oxide samples. The total conversion is always increased; this enhancement is relatively low on the high-surface sample (La_2O_3 ex-ammonia) whose specific area decreases with running time. On the other hand, on the small surface oxide (La_2O_3-hydrazine) an increased area is observed and hence the reactivity rises more rapidly than for the high surface samples.

After reaction, X-ray data show an evolution toward the formation of $La(OH)_3$ and probably of its carbonated form $La(OH)_x(CO_3)_{3-x}$. In the case of yttria catalyst, the compound formed will be $La_xY_{1-x}(OH)_3$, and its partially carbonated form.

As indicated in Fig. 2, the morphology is also modified during the CO–H_2 reaction.

Finally, the reactivity results are less related to the

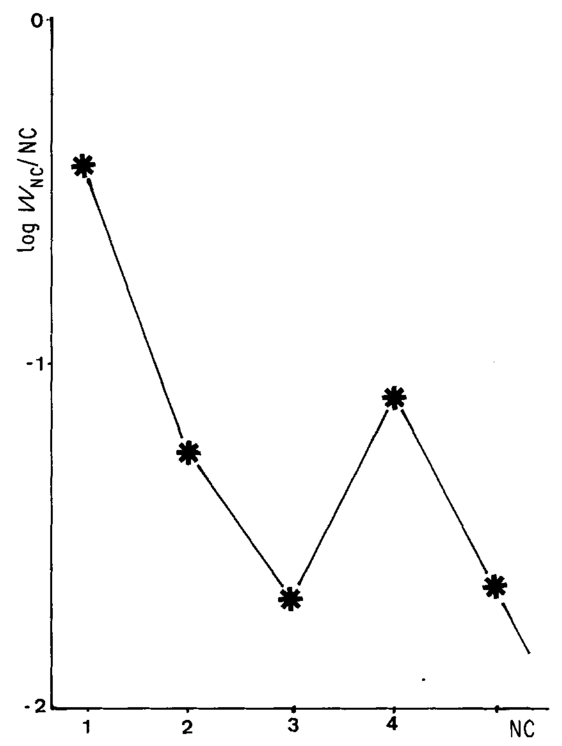

Figure 13 Product distribution of CO + H_2 reaction on La_2O_3 ex-ammonia activated at 550° C (weight fraction/carbon number).

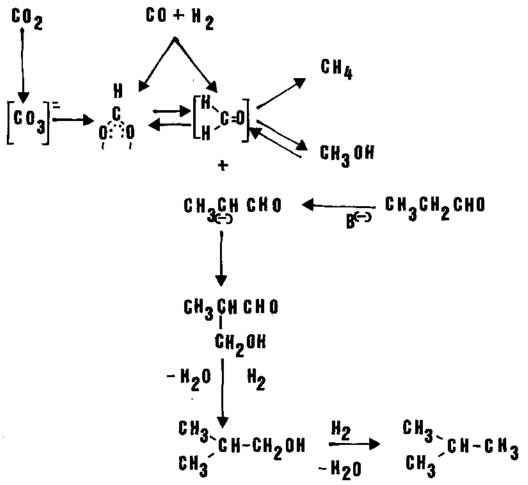

Figure 14 Schematic representation of the possible hydrogenation of carbonates to formates.

TABLE IV Reactivity of lanthana in the CO–H_2 reaction: effect of the pretreatment temperature

Catalyst	Area ($m^2\,g^{-1}$)	Conversion (%)			Selectivity RH					Selectivity ROH			Ratio iso C_4/C_4 (%)	Conversion iso C_4 (%)
		RH	ROH + DME	CO_2	C_1	C_2	C_3	C_4	C_5^+	DME	CH_3OH	iC_4OH		
La_2O_3 ex-ammonia 550° C	22	12.2	2.5	21.1	20	11	7	34	11	14	3	< 1	74	3.7
La_2O_3 ex-ammonia 800° C	5	6.8	0.8	10	25	14	13	22	15	9	1	< 1	67	1.2
La_2O_3 ex-ethoxy 600° C	1.4	6.4	1.1	9.1	32	13	11	27	2	4	8	3	75	1.6
La_2O_3 ex-ethoxy 710° C	4	5.5	1.3	8.6	23	11	14	28	5	12	5	1	74	1.5
La_2O_3 ex-ethoxy 800° C	4	4	1.6	7.7	19	14	9	23	7	15	9	4	62	1

P = 400 bar; T = 475° C; CO/H_2 = 1; G.S.V.H. = 2000; time 24 h; pretreatment, indicated with the catalyst preparation.

TABLE V Reactivity of lanthana in the CO–H_2 reaction: effect of addition of yttria

Catalyst	Conversion (%)			Selectivity RH					Selectivity ROH			Ratio iso C_4 / C_4 (%)	Conversion iso C_4 (%)
	RH	ROH	CO_2	C_1	C_2	C_3	C_4	C_5^+	DME	C_1OH	iC_4H_9OH		
La_2O_3 ex-ammonia 550° C	12.2	2.5	21.1	20	11	7	34	11	14	3	1	74	3.7
Y_2O_3 ex-ammonia 700° C	9.5	3.6	12.7	28	9	7	25	5	18	8	1	75	2.8
$0.8La_2O_3$–$0.2Y_2O_3$/550° C	9.8	2.1	14.6	24	9	2	31	16	11	5	< 1	75	2.9
$0.5La_2O_3$–$0.5Y_2O_3$/680° C	15.5	1.4	20.6	35	22	12	14	9	4	3	< 1	57	1.5

P = 400 bar; T = 475° C; CO/H_2 = 1; G.S.V.H. = 2000; time 24 h; pretreatment, indicated with the catalyst preparation.

nature of the precursor than to the thermal pretreatment and to the ageing of the catalysts. The best results are obtained after a pretreatment between 550 and 600° C.

These results are in accordance with the presence on these samples of formate and carbonate species. FT–IR spectra have evinced the possibility of hydrogenation of carbonates to formates. These intermediates led, through a well-established process, either to formaldehyde [30], which induces a chain growth by aldol condensation [8, 9, 31], or to methanol or methane [32] which are also observed in the reaction products (see Fig. 14).

4. Conclusions

The original low-temperature preparation allows the stabilization of the cubic form of La_2O_3 by the addition of Y_2O_3. The physical properties, morphology, specific area and chemisorption of probe molecules are influenced by the preparation and the pretreatment of the oxides.

The chemisorption of CO_2, on the different samples, gives carbonates with different stabilities. The adsorption of methanol in both linear and bridged configuration as well as the reduction of carbonates into formates as evinced by FT–IR spectroscopy, depends on the oxide preparation methods.

In CO–H_2 reactions, the prepared lanthana catalysts have a good activity in hydrocarbon and oxygenated formation. A particular distribution favouring iso C_4 compounds is observed.

In the hard reaction conditions used, the crystalline structure (hexagonal or cubic) and the preparation methods have an influence on the initial activity of the catalyst, but not on the evolution of the oxides to hydrates or carbonates during the synthesis.

Acknowledgement

We acknowledge the financial support of the Centre National de la Recherche Scientifique (CNRS) (A.T.P. No. 2260).

References

1. Y. IMIZU, K. SATO and H. HATTORI, *J. Catal.* **76** (1982) 65.
2. T. YAMAGUCHI, N. IKEDA, H. HATTORI and K. TANABE, *ibid.* **67** (1981) 324.
3. M. P. ROSYNEK, *Catal. Rev.* **16** (1977) 111.
4. H. PICHLER and K. H. ZIESECKE, *Brennstoff Chemie* **30** (1949) 13.
5. *Idem, ibid.* **30** (1949) 60.
6. *Idem, ibid.* **30** (1949) 81.
7. *Idem, ibid.* **39** (1949) 333.
8. R. KIEFFER, J. VARELA and A. DELUZARCHE, *J. Chem. Soc. Chem. Commun.* (1983) 763.
9. R. KIEFFER, G. CHERRY and R. EL. BACHA, *Cl. Mol. Chem.* **2** (1987) 11.
10. M. ICHIKAWA, *Bull. Chem. Soc. Jpn* **51** (1978) 2273.
11. *Idem, ibid.* **51** (1978) 2278.
12. *Idem, J. Catal.* **59** (1979) 67.
13. F. SOLYMOSI, M. PASZTOR and G. RAKHELY, *J. Catal.* **110** (1988) 413.
14. A. KIENNEMANN, R. BREAULT, J. P. HINDERMANN and M. LAURIN, *J. Chem. Soc. Farad. Trans. I* **83** (1987) 2119.
15. M. P. ROSYNEK and D. T. MAGNUSON, *J. Catal.* **46** (1977) 402.
16. D. TOURET and F. QUEYNOUX, *Rev. Chim. Min.* **9** (1972) 883.
17. M. D. MITTCHEL and M. A. VANNICE, *Ind. Eng. Chem. Fundam.* **23** (1984) 88.

TABLE VI Reactivity of lanthana in the CO–H_2 reaction: influence of ageing

Catalyst	Area ($m^2 g^{-1}$)	t (h)	Conversion (%)			Selectivity RH					Selectivity ROH			Ratio iso C_4 / C_4 (%)	Conversion iso C_4 (%)
			RH	ROH + DME	CO_2	C_1	C_2	C_3	C_4	C_5^+	DME	C_1OH	iC_4OH		
La_2O_3 ex-ammonia 550° C	22	24	12.2	2.5	21.1	20	11	7	34	11	14	3	< 1	74	3.7
		46	12.9	2.9	19.5	21	11	6	35	9	14	4	< 1	70	3.6
	15	70	13.6	2.8	20.7	24	10	5	34	10	11	5	< 1	76	4.3
La_2O_3-hydrazine 440° C	3	24	5.2	1.6	9.5	19	12	7	29	9	11	9	3	74	1.7
		45	8.5	2	12.4	20	11	8	35	7	12	6	1	71	2.7
		68	9.6	2.4	14.1	23	10	4	36	6	13	6	1	72	3.3
	10	92	11.1	2	15.4	27	12	8	35	3	11	4	< 1	72	3.3

P = 400 bar; T = 475° C; CO/H_2 = 1; G.S.V.H. = 2000; time 550 and 440° C.

18. S. BERNAL, J. A. DIAZ, R. GARCIA and J. RODRIGUEZ-IZQUIERDO, *J. Mater. Sci.* **20** (1985) 537.
19. S. BERNAL, F. J. BOTANA, R. GARCIA and J. RODRIGUEZ-IZQUIERDO, *React. Solids* **4** (1987) 23.
20. A. DELUZARCHE, J. P. HINDERMANN, A. KIENNEMANN and R. KIEFFER, *J. Mol. Catal.* **31** (1985) 225.
21. V. LORENZELLI and G. BUSCA, *Mater. Chem.* **7** (1982) 89.
22. S. BERNAL, S. J. BOTANA, R. GARCIA and J. RODRIGUEZ-IZQUIERDO, *Thermochim. Acta* **60** (1983) 139.
23. S. BERNAL, S. J. BOTANA, J. PINTADO, R. GARCIA and J. RODRIGUEZ-IZQUIERDO, *J. Less Common Met.* **110** (1985) 433.
24. S. BERNAL, F. J. BOTANA, R. GARCIA, F. RAMIREZ and J. RODRIGUEZ-IZQUIERDO, *J. Mater. Sci.* **22** (1987) 1517.
25. R. ALVERO, J. A. ODRIOZOLA, J. M. TRILLO and S. BERNAL, *J. Chem. Soc. Dalton Trans.* (1984) 87.
26. X. MONTAGNE, J. LYNCH, E. FREUND, J. LAMOTTE and J. C. LAVALLEY, *J. Chem. Soc. Farad. Trans. I* **83** (1987) 1417.
27. M. BENSITEL, V. MORAVEK, J. LAMOTTE, D. SAUR and J. C. LAVALLEY, *Spectrochim. Acta* **43A** (1987) 1487.
28. J. LAMOTTE, V. MORAVEK, M. BENSITEL and J. C. LAVALLEY, *React. Kinet. Catal. Lett.*, **36** (1988) 113.
29. P. CHAUMETTE, Ph. COURTY, J. BARBIER, T. FORTIN, J. C. LAVALLEY, C. CHAUVIN, A. KIENNEMANN and H. IDRISS, Proceedings of the 9th International Congress on Catalysis, Calgary, 1988, edited by M. J. Phillips and M. Ternan, Vol. 2 (1988) 585.
30. J. P. HINDEMANN, A. DELUZARCHE, R. KIEFFER and A. KIENNEMANN, *Can. J. Chem. Engng* **61** (1983) 21.
31. R. KIEFFER, G. CHERRY, J. VARELA and R. TOUROUDE, *J. Chim. Phys.* **84** (1987) 901.
32. R. STUPFLER, A. DELUZARCHE, R. KIEFFER and A. KIENNEMANN, *Cl. Mol. Chem.* **1** (1985) 179.

Received 18 April
and accepted 7 September 1988